Journal of Physics: Conference Series **1342** (2020) 012030 doi:10.1088/1742-6596/1342/1/012030

Testing the Neutrino Mass Ordering with Four Years of IceCube/DeepCore Data

Martin Leuermann (for the IceCube Collaboration)

III. Physikalisches Institut B, RWTH-Aachen University, Otto-Blumenthal Str., 52074 Aachen, Germany

E-mail: leuermann@physik.rwth-aachen.de

Abstract. The measurement of the Neutrino Mass Ordering (NMO), i.e. the ordering of the neutrino mass eigenstates, is one of the major goals of many future neutrino experiments. One strategy is to measure matter effects in the oscillation pattern of atmospheric neutrinos as proposed for the PINGU extension of the IceCube Neutrino Observatory. Already, the currently running IceCube/DeepCore detector can explore this type of measurement. Albeit with lower significance, such a measurement can contribute to the current understanding. Furthermore, such an analysis exercises the measurement principle and evaluation of systematic uncertainties and thus prototypes future analyses with PINGU. We present a likelihood analysis spanning multiple years of IceCube data searching for indications of the NMO with a data sample reaching to energies below 10 GeV.

1. Introduction

The Neutrino Mass Ordering (NMO) describes the energetic ordering of the three neutrino mass eigenstates. Depending on the sign of the squared-mass difference Δm^2_{13}, one refers to Normal Ordering (NO) or Inverted Ordering (IO) for positive or negative values, respectively. Depending on the NMO, matter effects in the neutrino oscillation pattern, such as the MSW-effect, arise in the neutrino or the anti-neutrino channel. The resulting modulation of the oscillation pattern can be observed in atmospheric neutrinos, that undergo matter effects during their propagation through the Earth, as proposed for the PINGU extension of the IceCube Neutrino Observatory [1].

Atmospheric neutrinos are produced in the Earth's atmosphere by interactions of primary cosmic rays with the atoms of the air, generating charged mesons. These mesons decay generating electron and muon neutrinos, which can propagate through the Earth and eventually be detected by an underground neutrino detector, such as IceCube. Due to the diameter of the Earth, the first oscillation minimum for vertically up-going neutrinos arises at $E_\nu \sim 25\,\mathrm{GeV}$, while this energy decreases with shorter baselines towards the horizon [2]. Matter effects allowing to determine the NMO arise mainly below $E_\nu \sim 15\,\mathrm{GeV}$. Although the oscillation pattern for neutrinos and anti-neutrinos are complementary and IceCube is not capable to distinguish neutrinos and anti-neutrinos on an event-by-event level, the NMO leads to a visible net-effect, as the cross-sections and thus the rates for neutrinos and anti-neutrinos are different [1].

2. The IceCube/DeepCore Detector

The IceCube Neutrino Observatory is a $\sim 1\,\mathrm{km}^3$ size neutrino detector at the Geographic South Pole, capable to detect atmospheric and astrophysical neutrinos down to $\sim 100\,\mathrm{GeV}$. It consists of 86 strings running through the ice vertically from the ice surface to near the bedrock, carrying 5160 Digital Optical Modules (DOMs) in depths between 1450 m and 2450 m. Each DOM houses a photomultiplier tube and digitizing electronics, surrounded by a glass sphere [3].

In the center of the detector, 8 strings form a more densly instrumented volume, called DeepCore. Due to the denser instrumentation and high quantum-efficiency DOMs, the DeepCore fill-in lowers the energy threshold to $\sim 5\,\mathrm{GeV}$ [3].

Neutrinos are detected by the Cherenkov emission of their charged secondary particles, which are generated by charged-Current (CC) and Neutral-Current (NC) interactions with the nucleons of the ice. In case of CC muon-neutrino interactions, the produced muon can propagate large distances through the detector, leading to an elonganted shape of the energy deposition and thus, of the light emission. Such events are called track-like signatures. In contrast, CC electron- or tau-neutrino and NC interactions do not produce a muon that can travel large distances. Instead, they initiate an electromagnetic and/or hadronic cascade of nearly spherical symmetry in light emission. Such events are called cascade-like [3, 1].

3. Data Sample and Reconstruction

To test the NMO in IceCube/DeepCore, two low-energy data samples and analyses were developed independently. Their main differences are summarized in Table 1, while the following focuses on Analysis A.

Table 1. Overview of the main differences in selection, reconstructed energy range, number of analysis bins and expected events per year for the two NMO analyses

Analysis	Selection	Energy Range	Bins $(E_\nu, \vartheta_\nu, \mathrm{PID})$	Events per Year	Years
Analysis A	high statistics	$4 - 90\,\mathrm{GeV}$	(10, 10, 3)	$\sim 22\,000$	4
Analysis B	quality events	$5 - 80\,\mathrm{GeV}$	(10, 5, 2)	$\sim 9\,000$	3

For the data sample, we use variables describing the topology of the event, its location and extension within the detector, its direction and its energy. After some pre-selection steps on these variables to reduce the amount of data, two subsequent Boosted Decision Trees (BDT) are used to reduce the background of atmospheric muons and triggered detector noise, while keeping a large fraction of well-reconstructable electron-, muon- and tau-neutrino events.

The resulting sample is reconstructed using a likelihood-based reconstruction, comparing the observed and expected number of photo-electrons in each DOM of the detector. The fitted hypothesis consists of a cascade at the primary vertex and an outgoing, minimum-ionizing track for which the length, and thus the track energy, is being fitted. Besides the cascade and the track energies, the vertex and the direction are being fitted. In a second step, the track-length is set to zero and the cascade-only hypothesis, nested in the cascade+track hypothesis, is being fitted. The likelihood difference between the two hypotheses (called PID) is used to distinguish the event signatures in the following binned likelihood analysis.

4. Testing the NMO in a Binned-Likelihood Analysis

The NMO is tested in a binned-likelihood analysis. Therefore, the reconstructed energy E_ν, zenith-angle ϑ_ν and PID estimator are binned in a three-dimensional histogram for experimental

data and for Monte Carlo simulations (MC). The resulting histograms for MC is shown in Figure 1. Several components contribute to this histogram of events: CC muon-neutrino

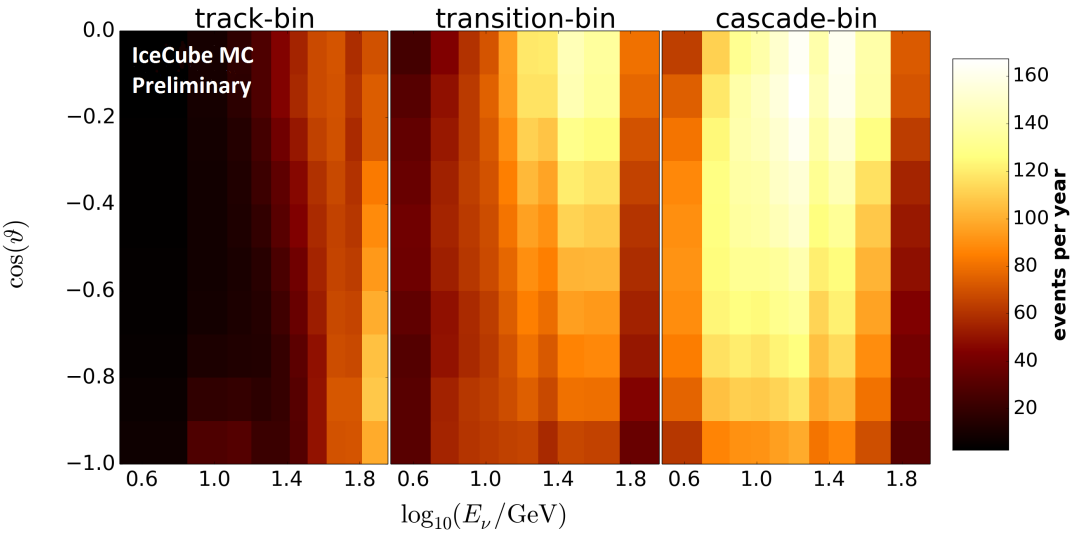

Figure 1. Three-dimensional MC histogram entering the likelihood analysis; the three PID bins are shown side by side and labeled according to their main content as track-, transition- and cascade-bin

interactions ($\sim$ 56%), CC electron-neutrino interactions ($\sim$ 22%), CC tau-neutrino interactions ($\sim$ 5%), NC interactions ($\sim$ 11%), atmospheric muons ($\sim$ 6%) and triggered detector noise ($\sim$ 0.1%), where the exact fractions depend on the realization of the nuisance parameters, discussed below, and the value in brackets is obtained for nominal nuisance parameters.

These histograms for data and MC are compared using a Poissonian likelihood, where the Poissonian is additionally convolved with a narrow Gaussian, describing the uncertainty on the bin-prediction due to the limited amount of MC simulations. This way, the uncertainty from limited MC statistics is included. Additionally, a Kernel Density Estimation (KDE) method is applied, to reduce the impact of statistical fluctuations on the MC template [5]. The NMO that optimizes this likelihood function is the one preferred by data.

In addition to testing the NMO, several nuisance parameters are fitted simultaneously. These nuisance parameters are derived by parametrizing the impact of each known systematic on the three dimensional histogram and then adding a corresponding parameter to the fitter. These nuisance parameters comprise oscillation parameters, detector systematics, flux- and cross-section uncertainties and are listed in Table 2. Additionally, some of the nuisance parameters are used with a Gaussian prior in the fitter. The width of the prior is motivated by external information and chosen to be larger or equal to our best knowledge of that parameter. The values for the priors and the baseline values are listed in Table 2.

Both hypotheses, NO and IO, are fitted for both octants, i.e. $\sin^2(\theta_{23}) \leq 0.5$ and $\sin^2(\theta_{23}) > 0.5$, separately. The best fit points for each of the two NMO are taken to calculate the log-likelihood-ratio $\Delta LLH = \log LH_{\mathrm{NO}} - \log LH_{\mathrm{IO}}$. Thus, $\Delta LLH < 0$ and $\Delta LLH > 0$ correspond to the fit preferring NO or IO, respectively.

5. Results

The sensitivity towards the NMO is estimated using the Asimov-approach described in [4]. It allows for a conversion of the observed ΔLLH into a sensitivity in terms of a significance for

Table 2. Systematics treated as nuisance parameters in the likelihood analysis, including normalization (N), detector-response (D), oscillation (O), flux (F) and cross-section (C) uncertainties, where Δ estimates the relevance of fitting the parameter to obtain an unbiased NMO result (s. Section 5 for details).

Label	Type	Description	Baseline±Prior	Δ (NO/IO)
N_e	N	normalization of electron-neutrino events	1 ± 0.1[a]	16%/69%
N_{NC}	N	normalization of NC events	1 ± 0.2[a]	9%/6%
N_μ	N	normalization of atmos. muon events	1[a]	19%/20%
ϵ_{PMT}	D	overall optical efficiency [3]	1 ± 0.1[a]	198%/161%
$L^{\mathrm{hi}}_{\mathrm{scat}}$	D	Scattering length in re-frozen holeice [3]	25 ± 10 cm	129%/144%
$L^{\mathrm{hi}}_{\mathrm{fwd}}$	D	head-on optical efficiency [3]	0[b]	80%/54%
Δm^2_{31}	O	atmos. squared-neutrino-mass difference	$2.5 \cdot 10^{-3}$ eV^2	-
θ_{23}	O	atmos. neutrino mixing angle	0.74 rad	-
γ_ν	F	neutrino spectral index unc. [7]	0.0 ± 0.1	48%/42%
γ_μ	F	atmospheric muon spectrum unc. [8]	0.0 ± 1.0[b]	1%/1%
$\sigma^{\mathrm{zenith}}_\nu$	F	zenith-dependent unc. in ν-flux [6]	0.0 ± 1.0[b]	142%/111%
$\Delta(\nu/\bar{\nu})$	F	energy-dependent unc. in $\nu/\bar{\nu}$-ratio [6]	0.0 ± 1.0[b]	121%/127%
M^{res}_A	C	axial mass unc. of resonant events [9]	1.12 ± 0.22 GeV	28%/3%
M^{qe}_A	C	axial mass unc. of quasi-elastic events [9]	0.99 ± 0.25 GeV	21%/22%

[a] relative to the nominal value of this parameter
[b] parametrized with respect to the value and the uncertainty obtained from the provided reference

both of the orderings. The resulting sensitivity for the Analyses A and B are shown in Figure 2 and 3 for the true ordering being NO and IO.

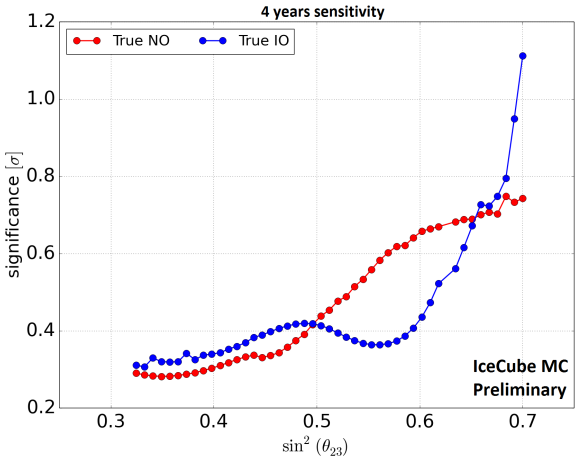

Figure 2. Sensitivity for Analysis A

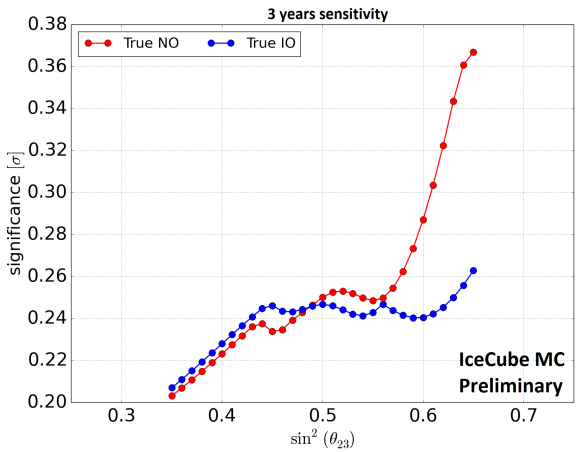

Figure 3. Sensitivity for Analysis B

Both analyses are in the regime of $0.25 - 0.55\,\sigma$ sensitivity in the most interesting region near maximum-mixing, while the high-statistics Analysis A reaches slightly higher values. The shape of the sensitivity curve arises from the fit of two octants for both hierarchies, leading to a flip of the preferred octant for the wrong ordering depending on the mixing angle θ_{23}.

Furthermore, the importance of the systematics is tested by fixing the corresponding parameter in the fitter to its baseline value. Then, the parameter is injected at $\pm 1\sigma$ off that

value and fitted for both orderings. This way, a systematically wrong hypothesis is fitted, that can not be corrected by the fitter, and its impact on fitting the NMO is tested. The resulting bias in the log-likelihood ratio, i.e. $\Delta^{\pm 1\,\sigma} = |(\Delta LLH_{\pm 1\,\sigma} - \Delta LLH_{\text{nominal}})/LLH_{\text{nominal}}|$, is averaged for $\pm 1\sigma$ and shown as Δ in Table 2 for NO and IO being true. It estimates the relevance of fitting the nuisance parameter to obtain an unbiased result: Parameters with large values in Δ must be fitted to not induce a bias in the obtained NMO, while small values allow to remove the corresponding parameter without biasing the outcome of the analysis. For parameters without priors, the width of $\pm 1\,\sigma$ was chosen motivated by its expected statistical uncertainty. In addition to the shown parameters, further systematics were investigated and removed, as their impact was negligible.

Note, that the atmospheric oscillation parameters are not tested in the above manner, since the NMO measurement is strongly coupled to the measurement of the oscillation parameters. For example, fixing the value of Δm^2_{31} also fixes the NMO, since the NMO is given only by the sign of Δm^2_{31}, while shifting θ_{23} by $\pm 1\sigma$ leads to a flip in the octant that also changes the interpretation of the obtained result.

As visible in Table 2, the detector uncertainties and uncertainties in the atmospheric neutrino flux are the most relevant systematics in testing the NMO with DeepCore.

6. Conclusion

We developed two independent analyses to test the Neutrino Mass Ordering on multiple years of IceCube/DeepCore data. The resulting sensitivity depends on the true mixing angle θ_{23} and the true NMO. It is in the $0.25 - 0.55\sigma$ range for the most interesting region close to maximum mixing.

The most relevant systematics for such a measurement are the uncertainties of the detector, namely the optical properties of the re-frozen hole ice and the efficiency of the photon detection, and the neutrino flux uncertainties. Thus, for a potential future measurement of the NMO with IceCube-Gen2 Phase I or PINGU, a more detailed description of the ice and the detector response is needed. Extending the current detector by new calibration devices to study the ice properties is a crucial effort for IceCube-Gen2 Phase I.

Although this result is of low significance, it contributes to the current understanding of the challenges of this analysis and probes the capability of a future low-energy extension to measure the NMO within IceCube.

References

[1] The IceCube-Gen2 Collaboration 2017 PINGU: a vision for neutrino and particle physics at the south pole *J. Phys.* G **44** 054006
[2] The Super-Kamiokande Collaboration 2016 Establishing atmospheric neutrino oscillations with Super-Kamiokande *Nucl. Phys.* B **908** 14
[3] The IceCube Collaboration 2009 The IceCube data acquisition system: signal capture, digitization, and timestamping *Nucl. Instrum. Meth.* A **601** 294
[4] Ciufolli E, Evslin J and Zhang X 2014 Confidence in a neutrino mass hierarchy determination *JHEP* **01** 095
[5] Wang B and Wang X 2007 Bandwidth selection for weighted kernel density estimation *arXiv:0709.1616v2*
[6] Barr G D, Gaisser T K, Robbins S and Stanev T 2006 Uncertainties in atmospheric neutrino fluxes *Phys. Rev.* D **74** 094009
[7] Honda M, Sajjad Athar M, Kajita T, Kasahara K, Midorikawa S 2015 Atmospheric neutrino flux calculation using the NRLMSISE00 atmospheric model *Phys. Rev.* D **92** 023004
[8] Evans J, Gamez D G, Porzio S D, Söldner-Rembold S, Wren S Uncertainties in atmospheric muon-neutrino fluxes arising from cosmic-ray primaries *arXiv:1612.03219*
[9] Andrepoulos C *et al.* 2010 The GENIE monte carlo generator *Nucl. Instrum. Meth.* A **640** 87 *Phys. Rev.* D **95** 023012